

We are IntechOpen, the world's leading publisher of Open Access books Built by scientists, for scientists

6,900

Open access books available

186,000

International authors and editors

200M

Downloads

Our authors are among the

154

Countries delivered to

TOP 1%

most cited scientists

12.2%

Contributors from top 500 universities



WEB OF SCIENCE™

Selection of our books indexed in the Book Citation Index
in Web of Science™ Core Collection (BKCI)

Interested in publishing with us?
Contact book.department@intechopen.com

Numbers displayed above are based on latest data collected.
For more information visit www.intechopen.com



Study on Influence of a State of Dopants on Dislocation-Dopant Ions Interaction in Annealed Crystals

Yohichi Kohzuki

Abstract

Combination method of strain-rate cycling tests and application of ultrasonic oscillations was conducted for KCl:Sr²⁺ (0.035, 0.050, 0.065 mol.% in the melt) single crystals at low temperatures. The measurement of strain-rate sensitivity (λ) of flow stress under the application of ultrasonic oscillatory stress provides useful information on the interaction between a mobile dislocation and impurities (Sr²⁺ ions) during plastic deformation and the variation of λ with stress decrement ($\Delta\tau$) due to oscillation has stair-like shape: The first plateau place ranges below the first bending point (τ_{p1}) at low stress decrement and the second one extends from the second bending point (τ_{p2}) at high stress decrement. The value of λ decreases with the $\Delta\tau$ between the two bending points. The τ_{p1} is considered to represent the effective stress due to impurities when a dislocation begins to break-away from the impurities with the help of thermal activation during plastic deformation. Annealing the impure crystal by heat treatment, τ_{p1} decreases obviously at low temperature and the critical temperature T_c , at which τ_{p1} is zero, also becomes slightly smaller. Furthermore, it was investigated whether a change in the state of a small amount of impurities has an influential factor of the flow parameters (e.g., the activation energy, the density of forest dislocations) from the data analyzed in terms of $\Delta\tau$ vs. λ curve.

Keywords: heat treatment, dislocation, ultrasonic oscillatory stress, activation energy, divalent ion

1. Introduction

A large number of investigations on strength of materials have been made with alkali halide crystals so far [1–4]. This will be because the crystals have some advantages [5]: A small number of glide systems on account of rock salt structure, low dislocation density in grown crystal (e.g., 10^4 cm^{-2} order for NaCl [6] and KCl [7] single crystals) as against that of annealed metals (around 10^7 cm^{-2} [8], e.g., 1 to $5 \times 10^6 \text{ cm}^{-2}$ in pure Cu single crystals [9], 1 to $5 \times 10^6 \text{ cm}^{-2}$ in α -brass single crystals [10], and 10^7 cm^{-2} order for pure Fe single crystals [11]), transparency, and further readily available single crystal, etc. Alkali halide crystals, therefore, are excellent materials for an investigation on mechanical properties of crystals.

When alkali halide crystals are doped with divalent impurities (divalent cations), the impurities induce positive ion vacancies in order to conserve the electrical neutrality and are expected to be paired with the vacancies. They are often at the nearest neighbor sites forming a divalent impurity-vacancy (I-V) dipole, which attract them strongly [12], for crystals quenched from a high temperature. Then asymmetrical distortions are produced around the I-V dipoles.

The greatest hardness occurs for the highest concentration of isolated I-V dipole and the decrease of hardness is attributed to precipitation in KCl:Sr²⁺ single crystals [13]. The state of impurities in a crystal affects its hardness. Chin et al. have obtained the following experimental results: KCl:Sr²⁺ (840 ppm) crystals soften on annealing at temperatures up to 773 K; the hardness of NaCl:Ca²⁺ (below 2000 ppm) crystals starts to increase rapidly after aging at 100 °C for 30 min and decreases on further annealing [14]. And also, it was reported that the change in their state strongly influences the resistance to movement of the dislocations when a small amount of impurities aggregates or diffuses into the crystal in various impure alkali halide crystals (e.g., NaCl: Ca²⁺ or Mn²⁺, KCl: Sr²⁺ or Ba²⁺, LiF:Mg²⁺) by heat treatment [15]. Annealing an impure crystal by heat treatment, this will lead to the change in various deformation characteristics.

Mobile dislocations on a slip plane interact strongly only with these defects lying within one atom spacing of the glide plane [16]. Dislocation motions are related to the plasticity of crystal in a microscopic viewpoint. Solution hardening depends on the dislocation motion hindered by the atomic defects around impurities in crystals and is namely influenced by the dislocation-point defects interaction. Annealing KCl:Sr²⁺ single crystals here, the study on the interaction between a dislocation and impurities was made by the combination method of strain-rate cycling tests and application of ultrasonic oscillations. This method seems to provide the information on dislocation-impurities interaction in ionic crystal during plastic deformation [17, 18].

2. Combination method of strain-rate cycling tests and application of ultrasonic oscillations

KCl:Sr²⁺ (0.035, 0.050, 0.065 mol.% in the melt) specimens were prepared by cleaving the single crystalline ingots to the size of 5 × 5 × 15 mm³. The specimens were kept immediately below the melting point for 24 h and were gradually cooled to room temperature at a rate of 40 K h⁻¹. This heat treatment was carried out for the purpose of reducing dislocation density as much as possible. Further, the specimens were held at 673 K for 30 min and were rapidly cooled by water-quenching in order to disperse the impurities (Sr²⁺) in the specimens immediately before the following tests. The specimen KCl:Sr²⁺ (0.050 mol.%) is termed the quenched specimen in this article.

The specimens were compressed along the <100> axis at 77 K to the room temperature and the ultrasonic oscillatory stress (τ_v) was intermittently superimposed in the same direction as the compression. The strain-rate cycling test under the ultrasonic oscillation is illustrated in **Figure 1**. Superposition of oscillatory stress causes a stress drop ($\Delta\tau$) during plastic deformation. The strain-rate cycling between strain-rates of $\dot{\epsilon}_1$ ($2.2 \times 10^{-5} \text{ s}^{-1}$) and $\dot{\epsilon}_2$ ($1.1 \times 10^{-4} \text{ s}^{-1}$) was performed keeping the stress amplitude of τ_v constant. Then, the variation of stress due to the strain-rate cycling is $\Delta\tau'$. The strain-rate sensitivity ($\Delta\tau'/\Delta\ln\dot{\epsilon}$) of the flow stress, which is given by $\Delta\tau'/1.609$, was used as a measurement of the strain-rate sensitivity (λ). The details was described in the article [19].

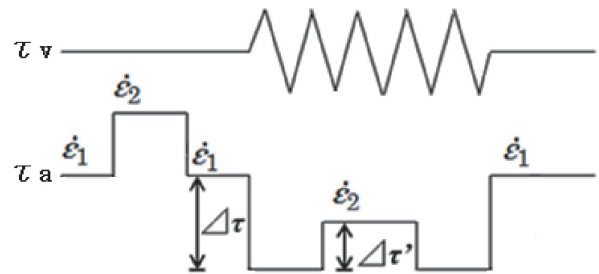


Figure 1.
Explanatory diagram of a change in applied shear stress, τ_a , for the strain-rate cycling test between the strain rates, $\dot{\epsilon}_1 (2.2 \times 10^{-5} s^{-1})$ and $\dot{\epsilon}_2 (1.1 \times 10^{-4} s^{-1})$, under superposition of ultrasonic oscillatory shear stress, τ_v .

3. Effective stress due to agglomerates in the crystals

Relation between $\Delta\tau$ and λ for $KCl: Sr^{2+}$ (0.050 mol.% in the melt) at the shear strain of 10% is shown in **Figure 2**. The measuring temperature is 103 K. $\Delta\tau$ vs. λ curve reflects the effect of ultrasonic oscillation on the dislocation motion on the slip plane containing many weak obstacles such as impurities and a few forest dislocations during plastic deformation [20]. Open circles in the figure represent the relation for the specimen quenched from 673 K to room temperature, and open triangles for the specimen obtained by storing the quenched specimen at room temperature for a half year. The second one is termed the stored specimen here. As can be seen from **Figure 2**, the variation of λ with $\Delta\tau$ has stair-like shape (there are two bending points on each curve, and there are two plateau regions: the first plateau region ranges below the first bending point (τ_{p1}) at low stress decrement and the second one extends from the second bending point (τ_{p2}) at high stress decrement) for the quenched specimen. λ

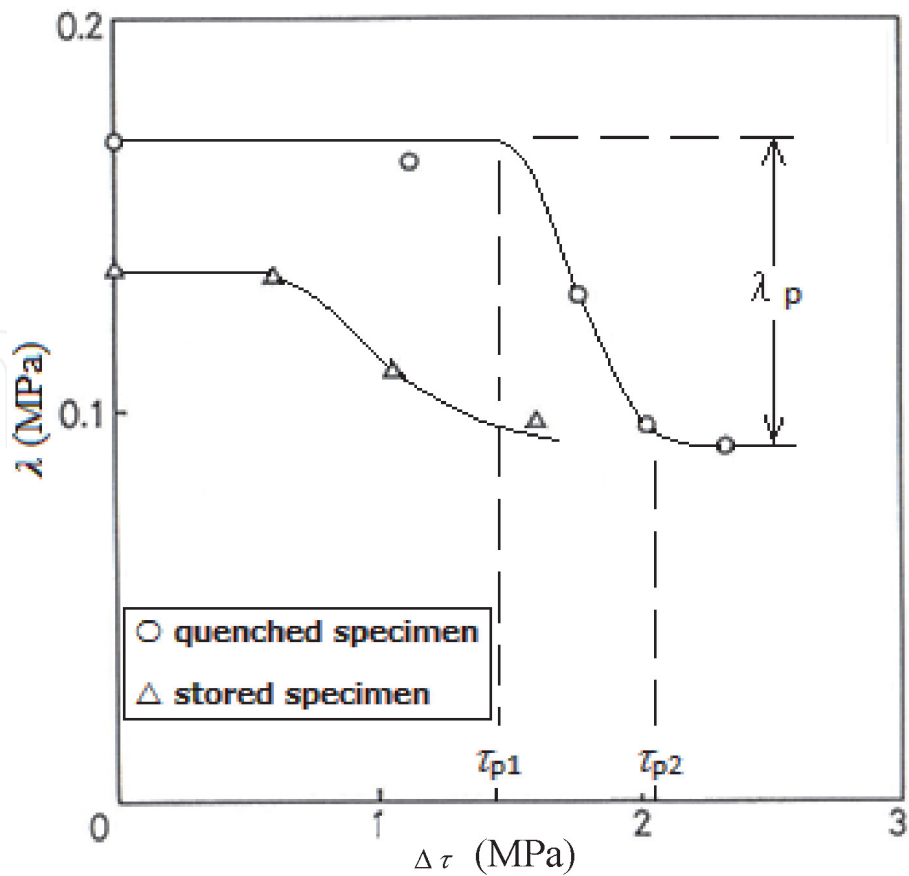


Figure 2.
Relation between the strain-rate sensitivity (λ) and the stress decrement ($\Delta\tau$) at 103 K for (\circ) the quenched specimen and (Δ) the stored specimen.

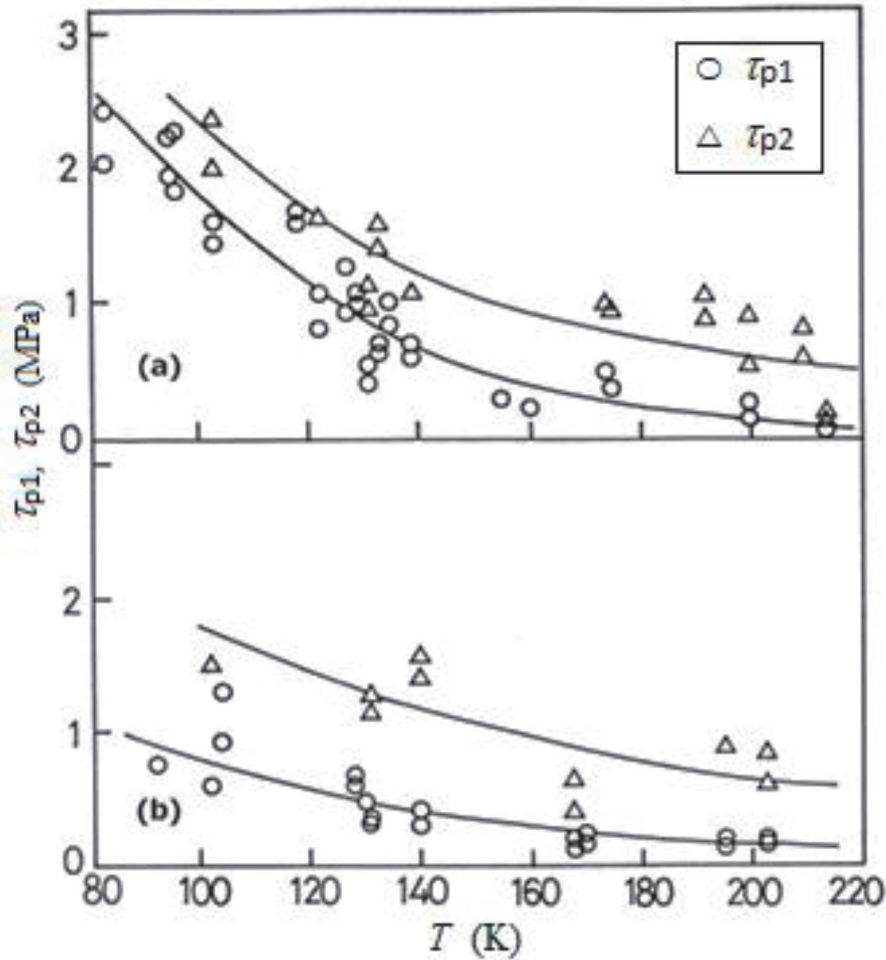


Figure 3. Dependence of (\circ) τ_{p1} and (Δ) τ_{p2} on temperature for (a) the quenched specimen and (b) the stored specimen.

decreases with the stress decrement between the two bending points. λ_p denoted in **Figure 2** is introduced in section 6 of this article. The τ_{p1} ($\Delta\tau$ value at the first bending point) for the stored specimen is smaller than that for the quenched specimen. τ_{p1} is considered to be the effective stress due to the impurities (Sr^{2+}) which lie on the dislocation when a dislocation begins to break-away from the impurities with the help of thermal activation during plastic deformation, because the value of τ_{p1} has been reported to be depend on temperature (τ_{p1} shifts in the direction of lower $\Delta\tau$ as the temperature becomes larger), and on the type and the density of weak obstacle [21]. The τ_{p2} ($\Delta\tau$ value at the second bending point) for the stored specimen, however, does not appear within the measurement, because high stress amplitude could not be applied to the specimen during the strain-rate cycling tests. Furthermore, τ_{p1} and τ_{p2} of the quenched and the stored specimens were investigated at various temperatures. **Figures 3(a)** and **(b)** show the results for the quenched specimen and for the stored one, respectively. The τ_{p1} for the stored specimen is smaller than that for the quenched specimen at a given temperature. On the other hand, the τ_{p2} for the stored specimen is a little smaller than that for the quenched one as compared with τ_{p1} . In the following sections of this article, the state of impurities in the specimen is clarified and its influence on the interaction between a dislocation and the impurities will be described.

4. State of impurities (Sr^{2+}) in $\text{KCl}:\text{Sr}^{2+}$ single crystals

Measurements of the I-V dipole concentration and of the flow stress for $\text{KCl}:\text{Sr}^{2+}$ (0.023 mol.%) were reported as a function of annealing time at 403 K after

quenching from 673 K by Dryden et al. [15]. Observing the concentration of isolated I-V dipoles in the crystal before and after the annealing and also the change of flow stress with it, the dipole concentration decreases and the flow stress becomes lower at a longer annealing time above 10 h.

Here is clarified the state of impurities in the specimen and is referred to the influence of the state of impurities on the dislocation-impurities interaction, especially on the relation between temperature and the effective stress. The crystals used here are two kinds of specimens. The first is KCl:Sr²⁺ (0.050 mol.% in the melt) at the preceding section 3 and is named the quenched specimen. The second is prepared by keeping the quenched specimen at 370 K for 500 h and gradually cooling in a furnace for the purpose of aggregating impurities in it [22]. This is hereafter termed the annealed specimen.

Dielectric absorption of an I-V dipole causes a peak on the tanδ-frequency relation. A relative formula which gives the proportionality between the concentration of I-V dipoles and a Debye peak height is expressed by [23].

$$\tan \delta = \frac{2\pi e^2 c}{3\epsilon' a k T}, (\text{maximum}) \tag{1}$$

where e is the elementary electric charge, c the concentration of the I-V dipole, ϵ' the dielectric constant in the matrix, a the lattice constant and kT has its usual meaning.

Figure 4 shows the influence of this heat treatment on the tanδ-frequency curves for KCl:Sr²⁺ at 393 K. The upper solid and dotted curves correspond to the

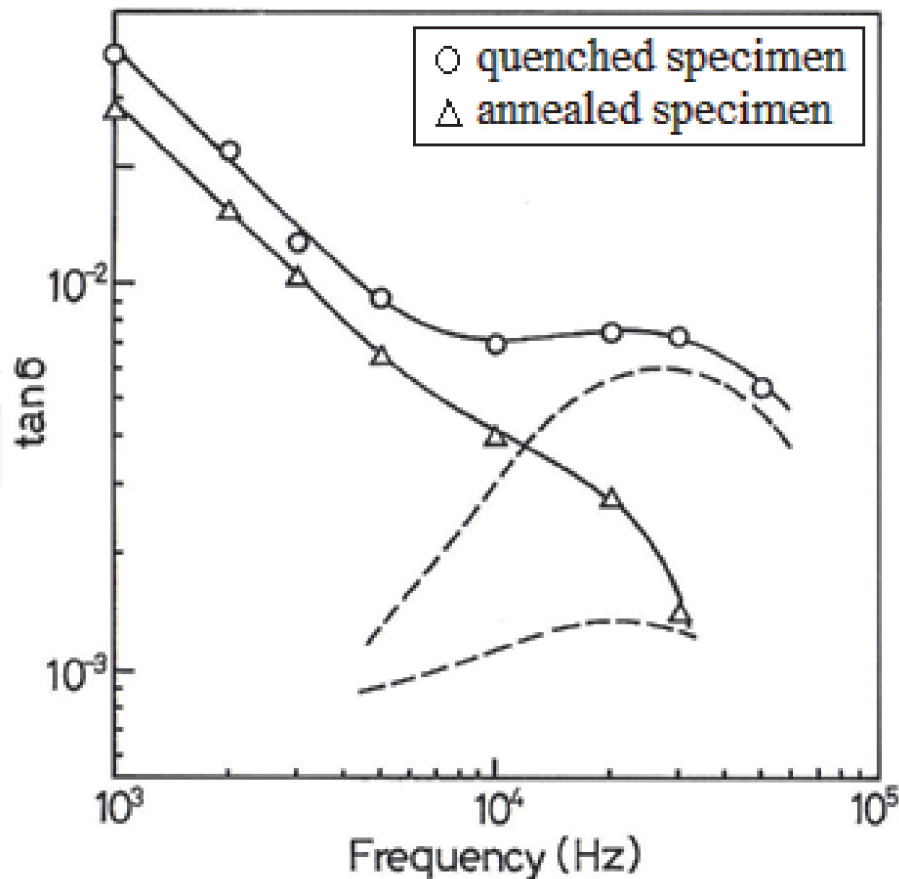


Figure 4. Dielectric loss in KCl:Sr²⁺ (0.050 mol.% in the melt) at 393 K: (○) for the quenched specimen, (Δ) for the annealed specimen. (---) losses coming from the dipoles (reproduced from ref. [24] with permission from the publisher).

quenched specimen and the lower curves the annealed specimen. Dotted lines show Debye peaks obtained by subtracting the d.c. part which is obtained by extrapolating the linear part of the solid curves in the low-frequency region to the high-frequency region. Introducing the peak heights of the dotted curves into Eq. (1), the concentration of the isolated dipole was determined to be 98.3 ppm for the quenched specimen and 21.8 ppm for the annealed specimen. On the other hand, the atomic absorption gave 121.7 ppm for the Sr^{2+} concentration in the quenched specimen and 96.2 ppm for the annealed specimen. Therefore, it should be considered that 71.9% of the I-V dipoles turn into the aggregates in $\text{KCl}:\text{Sr}^{2+}$ single crystal and form at least trimers [22] by the heat treatment. The trimers (Sr^{2+} -vacancy- Sr^{2+} -vacancy- Sr^{2+} -vacancy) have a structure in which three dipoles are arranged hexagonally head to tail in a (111) plane, as suggested by Cook and Dryden [22].

5. Effective stress and critical temperature

Figure 5 shows the variation of λ with $\Delta\tau$ at a shear strain of 8% for the annealed specimen at 125 K. The curve in the **Figure 5** has two bending points and two plateau regions at a given shear strain and temperature. The first plateau region ranges below the first bending point at low stress decrement and the second one extends from the second bending point at high stress decrement. The λ decreases with the $\Delta\tau$ between the two bending points. The values of $\Delta\tau$ at the first and the second bending points are referred to as τ_{p1} and τ_{p2} , respectively.

The dependence of τ_{p1} and τ_{p2} on temperature for the quenched specimen is shown in **Figure 6(a)**, while that for the annealed specimen is shown in **Figure 6(b)**. The value of τ_{p1} becomes small by forming into the aggregates in the crystal and this result is clearer at lower temperature. This may be caused by the result that the separation between the weak obstacles lying on the mobile dislocation becomes wider as the I-V dipoles turn into aggregates. In addition, it is supposed that the decrease in τ_{p1} due to agglomerate of the I-V dipoles, i.e. softening, would be attributable to the loss of tetragonality in terms of the Fleischer's model [16], as suggested by Chin et al.

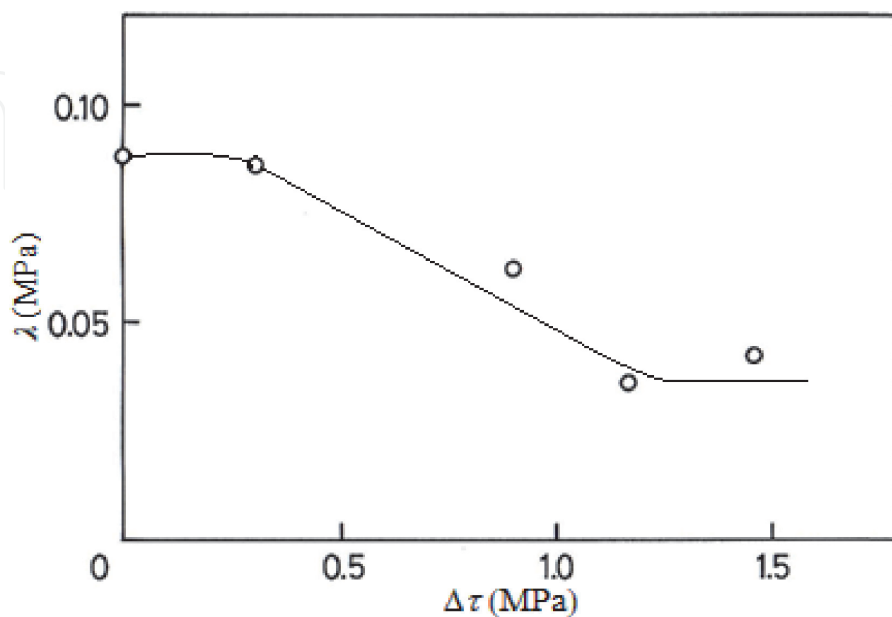


Figure 5. Relation between the strain-rate sensitivity (λ) and the stress decrement ($\Delta\tau$) at a shear strain of 8% for the annealed specimen at 125 K (reproduced from ref. [24] with permission from the publisher).

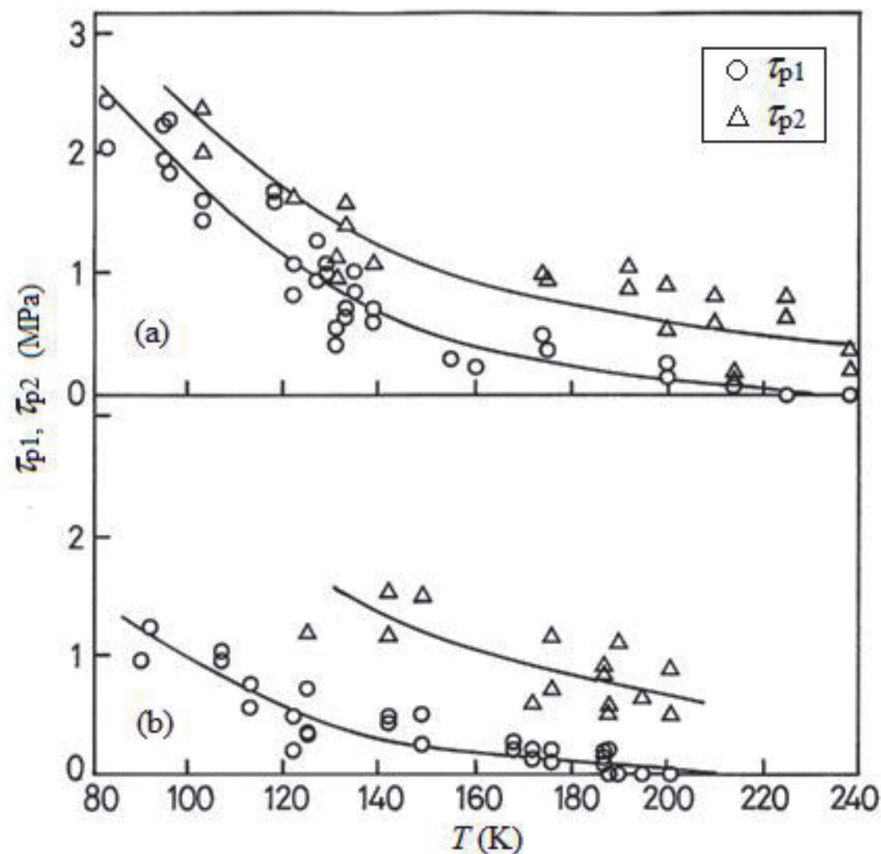


Figure 6.
Dependence of (○) τ_{p1} and (Δ) τ_{p2} on temperature for $\text{KCl}:\text{Sr}^{2+}$ (0.050 Mol.% in the melt): (a) for the quenched specimen and (b) for the annealed specimen (reproduced from ref. [24] with permission from the publisher).

[14]. The decrease in the effective stress due to agglomerates of I-V dipoles has been reported for alkali halide crystals doped with divalent cations so far [14, 15, 25–27].

As for τ_{p2} , no great difference is seen for the two kinds of specimens. Accordingly, as the I-V dipoles turn into the aggregates by the heat treatment, the difference between τ_{p1} and τ_{p2} obviously becomes wider at lower temperature. This may be caused by the wider distribution of Sr^{2+} obstacles on mobile dislocation in the annealed specimen as against that in the quenched one.

The critical temperature T_c at which τ_{p1} is zero and a dislocation breaks away from the impurities only with the help of thermal activation is around 210 K for the annealed specimen. This T_c value is small in contrast to $T_c \approx 240$ K of the quenched specimen as can be seen from **Figures 6(a)** and **(b)**.

6. Activation energy for the dislocation breaking-away from the defects

The thermally activated deformation rate ($\dot{\epsilon}$) is expressed by an Arrhenius-type equation:

$$\dot{\epsilon} = \dot{\epsilon}_0 \exp \left(\frac{-\Delta G}{kT} \right), \quad (2)$$

where $\dot{\epsilon}_0$ is a frequency factor and is unique for a particular dislocation mechanism. And the change in Gibbs free energy, ΔG , is expressed for square force-distance relation (SQ) between a dislocation and an impurity as follows.

$$\Delta G = \Delta G_0 - \tau^* L b d, \quad (3)$$

where ΔG_0 is the Gibbs free energy for the break-away of the dislocation from the impurity in the absence of an applied stress, τ^* the effective shear stress due to the impurities, L the length of dislocation, b the magnitude of the Burgers vector and d the activation distance. The Gibbs free energy for the SQ is given by

$$\Delta G = \Delta G_0 - \beta \tau^{*2/3} \quad (4)$$

$$\beta = (2\mu b^4 d^3 L_0^2)^{1/3}, \quad (5)$$

where μ is the shear modulus and L_0 the average spacing of impurities on the slip plane. Differentiating the substitutional equation of Eqs. (4) and (5) in Eq. (2) with respect to the shear stress, we find

$$\tau_{p1} \left(\frac{\partial \ln \dot{\epsilon}}{\partial \tau^*} \right) = \left(\frac{2\Delta G_0}{3kT} \right) + \frac{2}{3} \ln \left(\frac{\dot{\epsilon}}{\dot{\epsilon}_0} \right). \quad (6)$$

The Gibbs free energy for the interaction between a dislocation and the impurity is expressed from the Eq. (2), namely

$$\Delta G = \alpha kT, \quad \left(\alpha = \ln \left(\frac{\dot{\epsilon}_0}{\dot{\epsilon}} \right) \right) \quad (7)$$

and the ΔG for the Fleischer's model [16] taking account of the Friedel relation [28] (F-F) is also expressed by

$$\Delta G = \Delta G_0 \left\{ 1 - \left(\frac{\tau^*}{\tau_0^*} \right)^{1/3} \right\}^2, \quad (\Delta G_0 = F_0 b) \quad (8)$$

where τ_0^* is the value of τ^* at absolute zero and F_0 the force acted on the dislocation at 0 K. It is well known that the Friedel relation [28] between the effective stress and the average length of dislocation segments can be applied to most weak obstacles to dislocation motion at low solute concentration. Differentiating the combination of Eqs. (7) and (8) with respect to the shear stress gives

$$\frac{\partial \ln \dot{\epsilon}}{\partial \tau^*} = \left(\frac{2\Delta G_0}{3kT\tau_0^*} \right) \left(\frac{\tau_0^*}{\tau^*} \right)^{2/3} \left\{ 1 - \left(\frac{\tau^*}{\tau_0^*} \right)^{1/3} \right\} + \frac{\partial \ln \dot{\epsilon}_0}{\partial \tau^*}. \quad (9)$$

Further, substituting the following Eq. (10) in Eq. (9) gives Eq. (11)

$$\left(\frac{\tau_{p1}}{\tau_{p0}} \right)^{1/3} = 1 - \left(\frac{T}{T_c} \right)^{1/2} \quad (10)$$

namely,

$$\frac{\partial \ln \dot{\epsilon}}{\partial \tau^*} = \left(\frac{2\Delta G_0}{3kT\tau_{p0}} \right) \left\{ 1 - \left(\frac{T}{T_c} \right)^{1/2} \right\}^{-2} \left(\frac{T}{T_c} \right)^{1/2} + \frac{\partial \ln \dot{\epsilon}_0}{\partial \tau^*}, \quad (11)$$

where τ_0^* is replaced by τ_{p0} (τ_{p1} value at absolute zero). Eq. (10) represents the relative formula of τ_{p1} and temperature, which will reveal the force-distance

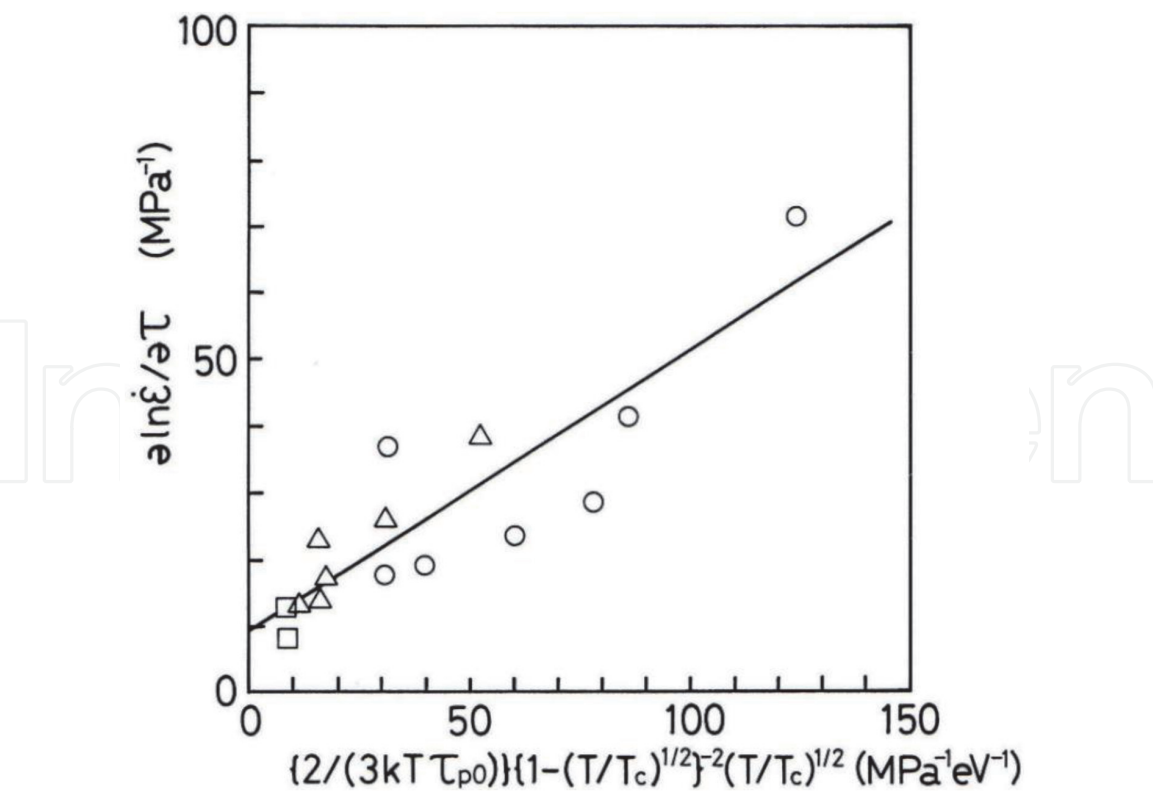


Figure 7.
Linear plots of Eq. (11) for the quenched specimen: $\text{KCl}:\text{Sr}^{2+}$ (\circ) 0.035 mol.%, (Δ) 0.050 mol.%, (\square) 0.065 mol.% in the melt) (reproduced from ref. [30] with permission from the publisher).

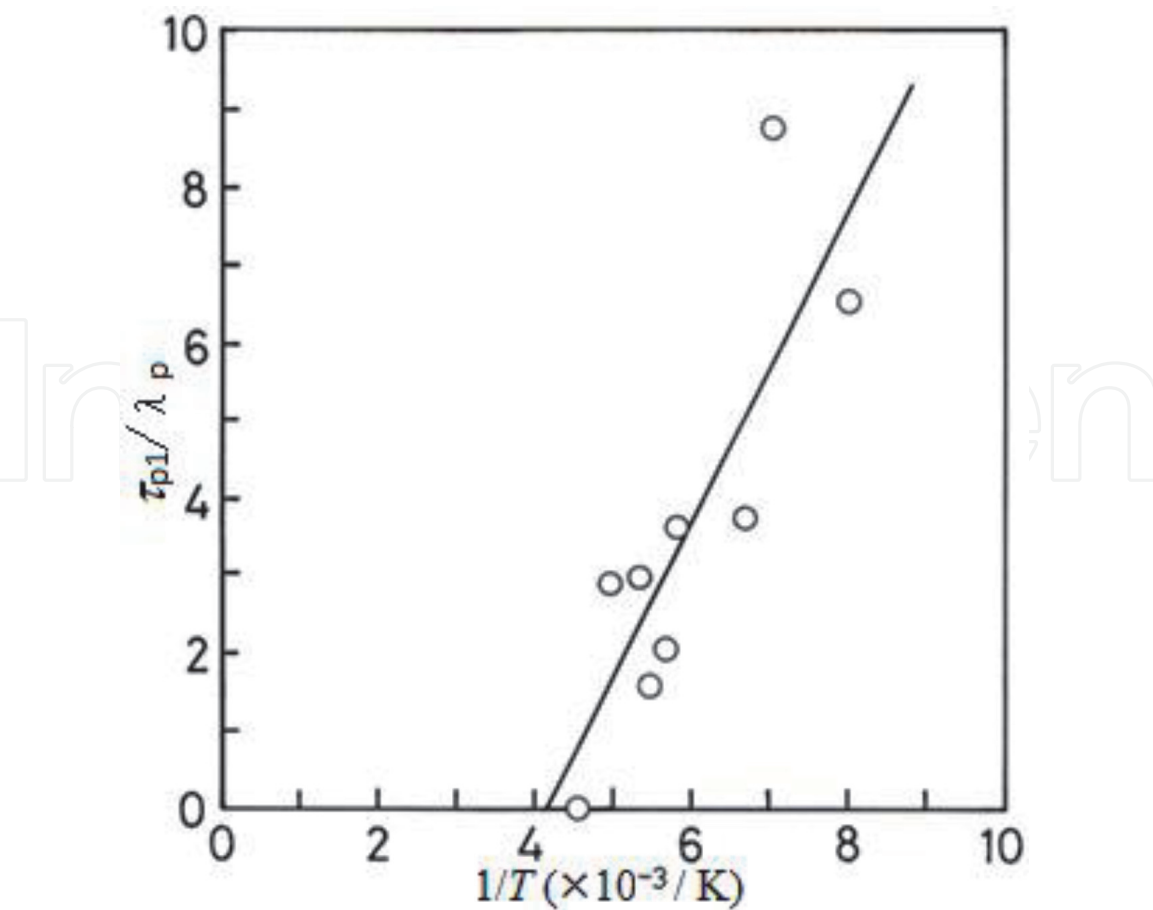


Figure 8.
Linear plots of Eq. (6) for the annealed specimen (reproduced from ref. [31] with permission from the publisher).

relation between a dislocation and an impurity. The result of calculations of Eq. (11) for the F-F is shown in **Figure 7** for the quenched specimen. The open symbols correspond to the inverse of λ_p for the quenched specimen, which are derived from the difference between λ values at first plateau place and at second one on the relative curves of $\Delta\tau$ vs. λ as shown in **Figure 2**. λ_p is considered to be due to the impurities [29]. On the basis of the slope of straight line, the Gibbs free energy is 0.39 eV. The F-F is suitable for the force-distance profile for the quenched specimen but not for the annealed one [30, 31]. As for the annealed specimen, SQ seems to be most suitable of the three profiles: a square force-distance relation, a parabolic one and a triangular one, taking account of the Friedel relation [31]. The Gibbs free energy for the interaction between a dislocation and the aggregate in the annealed specimen, which is obtained through the slope of straight line in **Figure 8**, is 0.26 eV. The open circles in **Figure 8** show the results of calculations for Eq. (6). Here, the $(\frac{\partial \ln \dot{\epsilon}}{\partial \tau^*})$ in Eq. (6) is obtained from λ_p . The Gibbs free energy for the annealed specimen is smaller than that of the quenched one.

7. λ at second plateau place on $\Delta\tau$ vs. λ curve

Influence of the heat treatment on the density of forest dislocations is treated in detail for the two kinds of KCl:Sr²⁺ (0.050 mol.% in the melt) single crystals (i.e., the quenched and the annealed specimens). This is examined from the variation of λ (see the marked part with gray circle in **Figure 9**) at the second plateau place on the $\Delta\tau$ vs. λ curve with shear strain, where the obstacles to the dislocation motion are only forest dislocations and the impurities no longer act as obstacles [21]. A general $\Delta\tau$ vs. λ at a given strain is schematically drawn in **Figure 9**, where the curve has two bending points and two plateau regions. The λ at second plateau place on the $\Delta\tau$ vs. λ curve is considered to be due to dislocation cuttings [21]. The variation of λ at second plateau place with shear strain ($\Delta\lambda/\Delta\epsilon$) is considered to be the increase of forest dislocation density with the shear strain [32]. In **Figure 10**, the $\Delta\lambda/\Delta\epsilon$ dependence of temperature is shown in the different plastic deformation regions of stress-strain curve for the two kinds of specimens: the quenched and the annealed

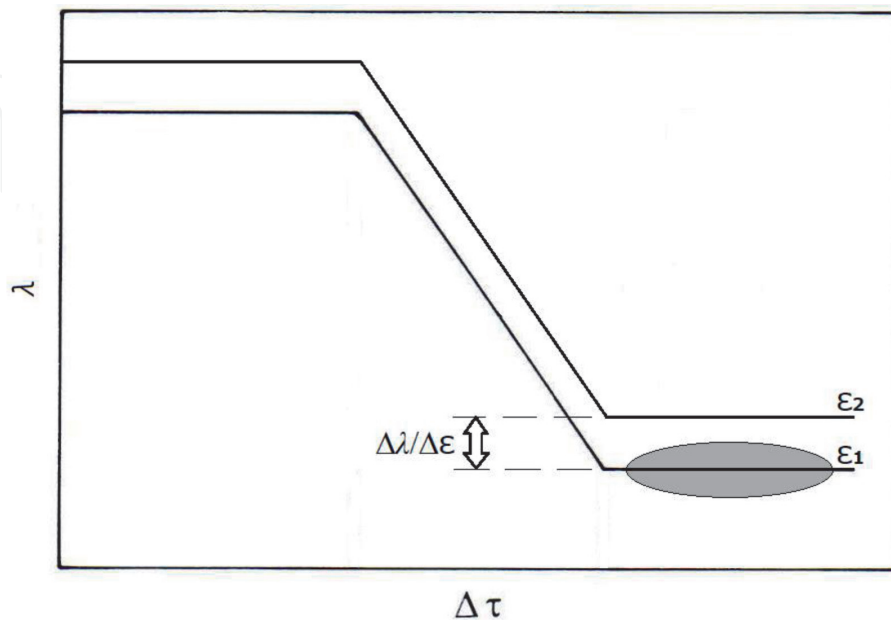


Figure 9. Illustration of relationship between the strain-rate sensitivity (λ) of flow stress and the stress decrement ($\Delta\tau$) at a given strain, ϵ . ($\epsilon_1 < \epsilon_2$).

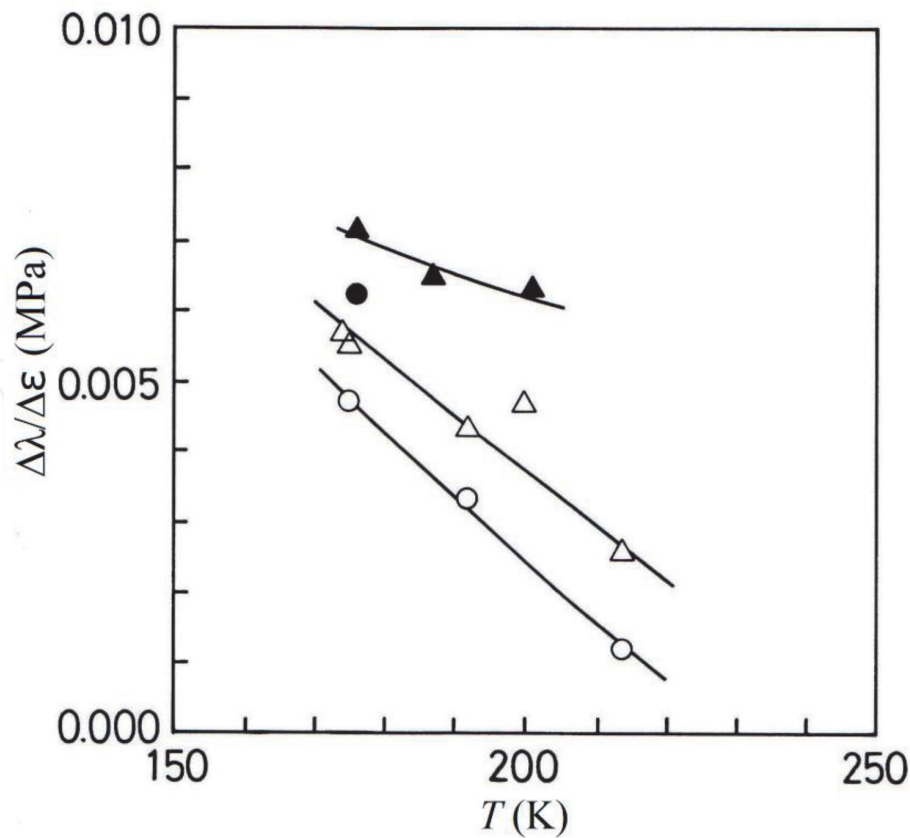


Figure 10.
Dependence of $\Delta\lambda/\Delta\epsilon$ on the temperature in the different plastic deformation regions: (\circ) for the quenched specimen and (\bullet) for the annealed specimen in stage I; (Δ) for the quenched specimen and (\blacktriangle) for the annealed specimen in stage II (reproduced from ref. [32] with permission from the publisher).

specimens. $\Delta\lambda/\Delta\epsilon$ in stage I (easy glide region) and in stage II (linear hardening region) are represented by a circle and a triangle, respectively. The open symbols correspond to that for the quenched specimen and the solid ones that for the annealed specimen. The curves in **Figure 10** are to guide the reader's eye. Unfortunately, the $\Delta\lambda/\Delta\epsilon$ could not be obtained at low temperature. Three-stage strain hardening is obtained for KCl [33, 34] and impure KCl single crystals doped with monovalent or divalent cations [35, 36]. Two phenomena are observed for both the specimens in **Figure 10**. That is, the first phenomenon is that the $\Delta\lambda/\Delta\epsilon$ in stage II is obviously larger than that in stage I at a given temperature. The other phenomenon is that the $\Delta\lambda/\Delta\epsilon$ in stage I and in stage II increases with decreasing temperature. **Figure 10** also shows that the $\Delta\lambda/\Delta\epsilon$ for the annealed specimens is considerably large in contrast to that for the quenched specimens in the two stages within the temperature. This may result from a rapid increase in forest dislocation density with shear strain in the annealed specimen. Accordingly, the increase in forest dislocation density in the annealed specimen seems to be remarkable in the two stages under the compression test, compared with it in the quenched specimen.

8. Conclusions

The following conclusions were derived from the data analyzed in terms of the $\Delta\tau$ vs. λ curves for KCl:Sr²⁺ single crystals.

1. The plots of $\Delta\tau$ vs. λ have two bending points and two plateau regions for the quenched specimen and similar result is observed also for the specimen stored at room temperature for a half year. On the basis of the relative curve of $\Delta\tau$ vs.

λ , it was found that τ_{p1} due to the impurities in the stored specimen is smaller than that of the quenched specimen within the temperatures.

2. The value of τ_{p1} becomes obviously smaller at lower temperature when I-V dipoles turn into the aggregates (trimers) in $\text{KCl}:\text{Sr}^{2+}$. This may be caused by the results that the separation between the Sr^{2+} obstacles lying on the mobile dislocation becomes wider, in addition to the loss of tetragonality in terms of the Fleischer's model, as the I-V dipoles turn into the agglomerates. By forming into the agglomerates in $\text{KCl}:\text{Sr}^{2+}$ single crystals, the value of T_c also becomes small.
3. The annealing treatment makes a difference in activation energy overcoming the impurity by a dislocation in the two kinds of $\text{KCl}:\text{Sr}^{2+}$ single crystals (quenched specimens and annealed ones). The value of $\Delta G_0 = 0.26$ eV is smaller for the dislocation motion in the annealed specimen, as compared with $\Delta G_0 = 0.39$ eV for the quenched specimen.
4. The variation of λ at the second plateau place on the curve of $\Delta\tau$ vs. λ with shear strain, i.e. $\Delta\lambda/\Delta\epsilon$, for the annealed specimen is considerably large in contrast to that for the quenched specimen in both stage I and stage II of stress-strain curve at 170 to 220 K. That is to say, the increase in forest dislocation density with shear strain for the annealed specimen seems to be remarkable in the two stages under the compression test, compared with that for the quenched specimen.

Conflict of interest

The author declares no conflict of interest.


Author details

Yohichi Kohzuki

Department of Mechanical Engineering, Saitama Institute of Technology, Fukaya, Japan

*Address all correspondence to: kohzuki@sit.ac.jp

IntechOpen

© 2021 The Author(s). Licensee IntechOpen. This chapter is distributed under the terms of the Creative Commons Attribution License (<http://creativecommons.org/licenses/by/3.0>), which permits unrestricted use, distribution, and reproduction in any medium, provided the original work is properly cited. 

References

- [1] Urusovskaya AA, Darinskaya EV, Voszka R, Jansky J. Defect structure and the nature of the obstacles for dislocations in NaCl(Ca) crystals. *Kristall und Technik*. 1981;16:597-601. DOI: <https://doi.org/10.1002/crat.19810160511>
- [2] Suszyńska M, Nowak-Woźny D. Mechanical characteristics of the NaCl: Eu²⁺ crystal system. *Crystal Research and Technology*. 1990;25: 855-861. DOI: <https://doi.org/10.1002/crat.2170250721>
- [3] Boyarskaya YS, Zhitaru RP, Palistrant NA. The anomalous behaviour of the doped NaCl crystals compressed at low temperatures. *Crystal Research and Technology*. 1990; 25:1469-1473. DOI: <https://doi.org/10.1002/crat.2170251219>
- [4] Sprackling MT. The plastic deformation of simple ionic crystals. In: Alper AM, Margrave JL, Nowick AS, editors. *Materials Science and Technology*. London New York San Francisco: Academic Press; 1976.
- [5] Kataoka T. Studies on plastic deformation of alkali halide crystals [thesis]. Osaka: Osaka University; 1975, p 2 (in Japanese).
- [6] Argon AS, Nigam AK, Padawer GE. Plastic deformation and strain hardening in pure NaCl at low temperatures. *Philosophical Magazine*. 1972;25:1095-1118. DOI: <https://doi.org/10.1080/14786437208226855>
- [7] Kohzuki Y. Studies on interaction between a dislocation and impurities in KCl single crystals [thesis]. Kanazawa: Kanazawa University; 1994, pp 12-13.
- [8] Suzuki H. Introduction to Theory of Dislocations. Tokyo: AGNE; 1989, p 70 (in Japanese).
- [9] Young Jr. FW. Etch pits at dislocations in copper. *Journal of Applied Physics*. 1961;32:192-201. DOI: <https://doi.org/10.1063/1.1735977>
- [10] Meakin JD, Wilsdorf HGF. Dislocations in deformed single crystals of alpha brass. I. General observations. *Transactions of the American Institute of Mining, Metallurgical and Petroleum Engineers*. 1960;218:737-745.
- [11] Takeuchi S. Solid-Solution Strengthening in Single Crystals of Iron Alloys. *Journal of the Physical Society of Japan*. 1969;27:929-940. DOI: <https://doi.org/10.1143/JPSJ.27.929>
- [12] Pick H, Weber H. Dichteänderung von KCl-Kristallen durch Einbau zweiwertiger Ionen. *Zeitschrift für Physik*. 1950;128:409-413. DOI: <https://doi.org/10.1007/BF01339441>
- [13] Green M. L, Zydzik G. Effect of heat treatment on the microhardness of some mixed and doped alkali halides. *Scripta Metall*. 1972;6:991-994. DOI: [https://doi.org/10.1016/0036-9748\(72\)90159-7](https://doi.org/10.1016/0036-9748(72)90159-7)
- [14] Chin G. Y, Van Uitert L. G, Green M. L, Zydzik G. J, Kometani T. Y. Strengthening of alkali halides by divalent-ion additions. *J. Am. Ceram. Soc*. 1973;56:369-372. DOI: <https://doi.org/10.1111/j.1151-2916.1973.tb12688.x>
- [15] Dryden J. S, Morimoto S, Cook J. S. The hardness of alkali halide crystals containing divalent ion impurities. *Philosophical Magazine*. 1965;12:379-391. DOI: <https://doi.org/10.1080/14786436508218880>
- [16] Fleischer RL. Rapid solution hardening, dislocation mobility, and the flow stress of crystals. *Journal of Applied Physics*. 1962;33: 3504-3508. DOI: <https://doi.org/10.1063/1.1702437>

- [17] Ohgaku T, Takeuchi N. The relation of the Blaha effect with internal friction for alkali halide crystals. *Physica Status Solidi A*. 1988;105:153–159. DOI: <https://doi.org/10.1002/pssa.2211050115>
- [18] Ohgaku T, Takeuchi N. Relation between plastic deformation and the Blaha effect for alkali halide crystals. *Physica Status Solidi A*. 1989;111:165–172. DOI: <https://doi.org/10.1002/pssa.2211110117>
- [19] Kohzuki Y. Study on dislocation-dopant ions interaction during plastic deformation by combination method of strain-rate cycling tests and application of ultrasonic oscillations. In: Singh D, Condurache-Bota S, editors. *Electron Crystallography*. IntechOpen: London; 2020. DOI: 10.5772/intechopen.92607
- [20] Kohzuki Y. Bending angle of dislocation pinned by an obstacle and the Friedel relation. *Philosophical Magazine*. 2010;90:2273–2287. DOI: 10.1080/14786431003636089
- [21] Kohzuki Y, Ohgaku T, Takeuchi N. Interaction between a dislocation and impurities in KCl single crystals. *Journal of Materials Science*. 1993;28:3612–3616. DOI: <https://doi.org/10.1007/BF01159844>
- [22] Cook J. S, Dryden J. S. An investigation of the aggregation of divalent cationic impurities in alkali halides by dielectric absorption. *Proceedings of the Physical Society*. 1962;80:479–488. DOI: 10.1088/0370-1328/80/2/315
- [23] Lidiard A. B. *Handbuch der Physik*, Berlin: Springer; 1957, Vol. 20, p 246.
- [24] Kohzuki Y, Ohgaku T, Takeuchi N. Influence of a state of impurities on the interaction between a dislocation and impurities in KCl single crystals. *Journal of Materials Science*. 1993;28:6329–6332. DOI: <https://doi.org/10.1007/BF01352192>
- [25] Johnston, W. G. Effect of Impurities on the Flow Stress of LiF Crystals. *Journal of Applied Physics*. 1962;33:2050–2058. DOI: <https://doi.org/10.1063/1.1728892>
- [26] Gaiduchenya V. F, Blistanov A. A, Shaskolskaya M. P. Thermally activated slip in LiF crystals. *Soviet Physics Solid State* 1970;12:27–31.
- [27] Buravleva M. G, Rozenberg G. K, Soifer L. M, Chaikovskii E. F. Changes in the flow stress of LiF:Mg²⁺ and LiF:Co²⁺ crystals during precipitation of solid solutions. *Soviet Physics Solid State*. 1980;22:150–152.
- [28] Friedel J. *Dislocations*, Oxford: Pergamon Press; 1964, p 224.
- [29] Kohzuki Y, Ohgaku T, Takeuchi N. Interaction between a dislocation and various divalent impurities in KCl single crystals. *Journal of Materials Science*. 1995;30:101–104. DOI: <https://doi.org/10.1007/BF00352137>
- [30] Kohzuki Y. Study on the interaction between a dislocation and impurities in in KCl:Sr²⁺ single crystals by the Blaha effect Part I Interaction between a dislocation and impurity for the Fleischer's model taking account of the Friedel relation. *Journal of Materials Science*. 2000;35:3397–3401. DOI: <https://doi.org/10.1023/A:1004889203796>
- [31] Kohzuki Y, Ohgaku T. Study on the interaction between a dislocation and impurities in in KCl:Sr²⁺ single crystals by the Blaha effect Part II Interaction between a dislocation and aggregates for various force-distance relations between a dislocation and an impurity. *Journal of Materials Science*. 2001;36:923–928. DOI: <https://doi.org/10.1023/A:1004807403566>
- [32] Kohzuki Y. Study on the interaction between a dislocation and impurities in KCl:Sr²⁺ single crystals by the Blaha

effect-Part IV influence of heat treatment on dislocation density. Journal of Materials Science. 2009;44: 379–384. DOI: <https://doi.org/10.1007/s10853-008-3150-8>

[33] Alden T. H. Latent hardening and the role of oblique slip in the strain hardening of rock-salt structure crystals. Transactions of the Metallurgical Society of AIME. 1964;230:649–656.

[34] Davis L. A, Gordon R. B. Plastic deformation of alkali halide crystals at high pressure: Work-hardening effects. Journal of Applied Physics. 1969;40: 4507–4513. DOI: <https://doi.org/10.1063/1.1657224>

[35] Kohzuki Y. Interaction between a dislocation and impurities in KCl doped with Li^+ or Na^+ . Journal of Materials Science. 2000;35:2273–2277. DOI: <https://doi.org/10.1023/A:1004735128091>

[36] Kohzuki Y. Influence of various divalent impurities on dislocation density in KCl:Mg^{2+} , Ca^{2+} , Sr^{2+} or Ba^{2+} single crystals. Journal of Materials Science. 2003;38:953–958. DOI: <https://doi.org/10.1023/A:1022373124795>